Exploring anti-fibrotic drugs

Luangmonkong, Theerut

Chapter A3

Human precision-cut liver slices as a model to test anti-fibrotic drugs in the early onset of liver fibrosis

Inge M. Westra[1,2], Henricus A.M. Mutsaers[2], Theerut Luangmonkong[2,3], Mackenzie Hadi[1], Dorenda Oosterhuis[2], Koert P. de Jong[4], Geny M.M. Groothuis[1], Peter Olinga[2,*]

[1] Department of Pharmacokinetics, Toxicology and Targeting, University of Groningen, the Netherlands

[2] Department of Pharmaceutical Technology and Biopharmacy, University of Groningen, the Netherlands

[3] Department of Pharmacology, Faculty of Pharmacy, Mahidol University, Thailand

[4] Department of Hepato-Pancreato-Biliary Surgery and Liver Transplantation, University Medical Center Groningen, University of Groningen, the Netherlands

* Corresponding author

Toxicology in Vitro 2016

Human precision-cut liver slices as a model to test anti-fibrotic drugs in the early onset of liver fibrosis

Abstract

Background and purpose

Liver fibrosis is the progressive accumulation of connective tissue ultimately resulting in loss of organ function. Currently, no effective anti-fibrotics are available due to a lack of reliable human models.

Experimental approach

Here we investigated the fibrotic process in human precision-cut liver slices (PCLS) and studied the efficacy of multiple putative anti-fibrotic compounds.

Key results

Our results demonstrated that human PCLS remained viable for 48h and the early onset of fibrosis was observed during culture, as demonstrated by an increased gene expression of heat shock protein 47 (HSP47) and pro-collagen 1A1 (PCOL1A1) as well as increased collagen 1 protein levels. SB203580, a specific inhibitor of p38-mitogen-activated protein kinase (MAPK) showed a marked decrease in HSP47 and PCOL1A1 gene expression, whereas specific inhibitors of SMAD3 and Rac-1 showed no or only minor effects. Regarding the studied anti-fibrotics, gene levels of HSP47 and PCOL1A1 could be down-regulated with sunitinib and valproic acid, while PCOL1A1 expression was reduced following treatment with rosmarinic acid, tetrandrine and pirfenidone. These results are in contrast with prior data obtained in rat PCLS, indicating that anti-fibrotic drug efficacy is clearly species-specific.

Conclusion and implications

Thus, human PCLS is a promising model for liver fibrosis. Moreover, MAPK signaling plays an important role in the onset of fibrosis in this model, and transforming growth factor beta pathway inhibitors appear to be more effective than platelet-derived growth factor pathway inhibitors in halting fibrogenesis in PCLS.

Key words: human precision-cut liver slices; liver fibrosis; anti-fibrotic; TGF-β.

Abbreviations: PCLS, precision-cut liver slices; TGF-β, transforming growth factor beta; PDGF, platelet-derived growth factor; MAPK, mitogen-activated protein kinase; HSP47, heat shock protein 47; αSMA, alpha smooth muscle actin; PCOL1A1, pro-collagen 1A1; GAPDH, glyceraldehyde-3-phosphate dehydrogenase; TIMP, tissue inhibitor of metalloproteinases; HDAC, histone deacetylase; ROS, reactive oxygen species.

Introduction

Fibrosis is an integral part of the pathophysiological mechanism of a diverse range of chronic diseases, such as Crohn's disease, chronic kidney disease and viral hepatitis. The fibrotic process is characterized by augmented production and excessive deposition of extracellular matrix proteins resulting in scar formation and the progressive loss of organ function. Liver cirrhosis, the end stage of liver fibrosis, is possibly the most clinically relevant form of tissue fibrosis in the world due to the high prevalence of viral hepatitis [1]. Consequently, liver fibrosis is widely studied, and there is extensive knowledge regarding the process of fibrogenesis [2]. And throughout the years a plethora of potential therapeutic targets have been described [3]. Nevertheless, an effective therapy for liver fibrosis remains elusive, and transplantation remains the sole successful treatment modality. Moreover, anti-fibrotic drug discovery is hampered by the lack of reliable and reproducible (human) *in vitro* models. Recently, precision-cut tissue slices have been used as a model for incipient and established fibrosis [4, 5]. Of note, this model replicates most of the multicellular characteristics of organs, and the different cells are retained in their original environment. Previously, rat and murine precision-cut liver slices (PCLS) have been successfully used to test the anti-fibrotic efficacy of several putative anti-fibrotic drugs [6-9]. Here we report the use of human PCLS to test anti-fibrotic compounds.

There are several well-known common signaling pathways involved in the fibrotic process in all organs, including the archetypical transforming growth factor beta (TGF-β) and platelet-derived growth factor (PDGF) pathways as well as the p38-mitogen-activated protein kinase (MAPK) pathway [1, 10, 11]. Even though these pathways are generally involved in fibrogenesis, there remain tissue-, species- and strain-specific differences [1, 12, 13]. In general, TGF-β signaling is associated with an increased deposition of collagen, whereas PDGF is a potent mitogen affecting cells of mesenchymal origin, such as myofibroblasts [10]. Both growth factors activate a myriad of transcription factors by binding to their respective receptors (*e.g.* type 1 TGF-β receptor or receptor tyrosine kinase) [14]. TGF-β acts mainly via SMAD signaling, which can be targeted by the specific inhibitor of SMAD3 (SIS3), known to inhibit TGF-β-induced SMAD3 phosphorylation [15]. PDGF stimulates cell proliferation via a host of downstream intracellular signaling cascades involving for instance glycogen synthase kinase 3β or Rho GTPases (*e.g.* Rac1). The latter can be specifically inhibited by NSC23766 [16]. MAPK is involved in the regulation of collagen 1A1 gene expression and mRNA stability, and can be activated by both PDGF and TGF-β [11]. SB203580 is a known inhibitor of MAPK [17]. Thus, next to studying the efficacy of anti-fibrotic compounds, the current study was also designed to identify the pathways underlying the (early) fibrotic response in healthy human PCLS using these pathway specific inhibitors.

Methods

Ethics statement

This study was approved by the Medical Ethical Committee of the University Medical Centre Groningen (UMCG), according to Dutch legislation and the Code of Conduct for dealing responsibly with human tissue in the context of health research (www.federa.org), refraining the need of written consent for 'further use' of coded-anonymous human tissue. The procedures were carried out in accordance with the experimental protocols approved by the Medical Ethical Committee of the UMCG.

Chemicals

All chemicals were obtained from Sigma Aldrich (Zwijndrecht, the Netherlands) unless stated otherwise. Stock solutions were prepared in either milli-Q or dimethyl sulfoxide (DMSO) and stored at −20 °C. During experiments, stocks were diluted in culture medium with a final solvent concentration of ≤1%.

Human liver tissue

Healthy human liver tissue was obtained either from patients following partial hepatectomy due to metastatic colorectal cancer (PH-livers) or from donors, remaining as surgical surplus after reduced-size liver transplantation (TX-livers), as described previously [18]. Clinical characteristics of study subjects who provided liver tissue are listed in Table 1. Of note, donor variability has limited impact on the fibrotic response in our model [19].

Table 1: Characteristics of liver donors.

Characteristic	Value
Source of liver tissue (number of PH/TX)	10/17
Sex (number of female/male)	20/7
Average age (range)	51 (10-82)

PH: tissue obtained from partial hepatectomy, TX: tissue obtained from transplantation liver.

Precision-cut liver slice preparation and experimental treatment

All liver tissue was perfused with cold University of Wisconsin (UW) organ preservation solution (DuPont Critical Care, Waukegan, IL, US) at the time of collection and stored in ice-cold UW solution until use [20]. Liver slices were prepared in ice-cold Krebs-Henseleit buffer supplemented with 25 mM D-glucose (Merck, Darmstadt, Germany), 25 mM $NaHCO_3$ (Merck), 10 mM HEPES (MP Biomedicals, Aurora, US) and saturated with carbogen (95% O_2/5% CO_2) using a Krumdieck tissue slicer as previously described [20]. In addition, slices were kept on ice-cold UW solution before culture, during which time viability and metabolic activity was maintained as described before [21].

PCLS (diameter: 5 mm, thickness: 250 µm) were incubated individually in 1.3 mL of Williams medium E (with L-glutamine, Invitrogen, Paisley, Scotland) supplemented with 25 mM glucose and 50 µg/mL gentamycin (Invitrogen) at 37 °C under continuous supply of 95% O_2/5% CO_2 in 12-wells plates while gently shaken. After 1h of preincubation, the slices were transferred to new plates with fresh medium and subsequently incubated for 24 or 48h in the presence or absence of anti-fibrotic compounds. Medium was refreshed every 24h. PCLS were treated with anti-fibrotics demonstrated to be effective in previous studies utilizing animal models, primary human cells and/or cell lines [7, 15, 22, 23] *i.e.* imatinib (Novartis, Basel, Switzerland), sorafenib (LC laboratories, Woburn, US), sunitinib (LC laboratories), perindopril, valproic acid, rosmarinic acid, tetrandrine, pirfenidone and the specific MAPK inhibitor SB203580 (Bio-Connect, Huissen, the Netherlands), the SMAD3 inhibitor SIS3 (Bio-Connect) and the Rac1 inhibitor NSC23766 (Tocris Bioscience, Bristol, UK). For the tested concentrations see Table 2, and to illustrate clinically relevant levels, the maximum serum concentration (Cmax) of compounds tested in humans is also provided. Furthermore, the PCLS were incubated with the growth factors PDGF-BB (10 and 50 ng/mL; Recombinant Human PDGF-BB; PeproTech, Bio-Connect) and TGF-β1 (1–5 ng/mL; hTGF-β1, Roche Applied Science, Mannheim, Germany). Non-specific binding of TGF-β1 was prevented by preincubating the culture plates with 10% BSA in milli-Q for 20 minutes, whereafter the solution was removed and plates were dried at room temperature. All experiments were performed in triplicate (technical replicates) using liver tissue from 3-5 different subjects.

Table 2: Experimental treatment.

Inhibitor	Compound	Concentration (µM)	Cmax (µM)
PDGF	Imatinib	1–10	5 [24]
	Sorafenib	0.5–2	9 [25]
	Sunitinib	0.5–5	14 [26]
TGF-β	Perindopril	10–100	0.04* [27]
	Valproic acid	100–1000	1000 [28]
	Rosmarinic acid	120–270	-
	Tetrandrine	1–10	-
	Pirfenidone	500–2500	85 [29]
SMAD3	SIS3	0.3–3	-
MAPK	SB203580	5–10	-
Rac1	NSC23766	5–50	-

*Perindoprilat is the active metabolite that inhibits angiotensin converting enzyme *in vivo*.

Histomorphological examination

Integrity of the slices was assessed by immunohistochemistry as previously described [30]. In short, PCLS were fixated with 70% ethanol at 4 °C for 24h, and subsequently rehydrated in successive baths of xylene and graded alcohols using a Shandon 2LE Processor. Afterwards, slices were vertically embedded in paraffin, sectioned (4 µm) and stained with hematoxylin and eosin. On microscopical examination, viability was determined by estimating the percentage of viable cells in the cross-section, taking nuclear shape/staining and cytoplasmatic staining into account.

ATP determination

The viability of the slices was determined by measuring ATP levels, as reported previously [31]. In short, following treatment, PCLS were transferred to 1 mL sonication solution, containing 70% ethanol and 2 mM EDTA, snap frozen in liquid nitrogen and stored at -80 °C until use. Subsequently, samples were thawed on ice, homogenized for 45 seconds using a Mini-BeadBeater-8 (BioSpec, Bartlesville, US) and centrifuged for 2 minutes at 16,000 g. ATP levels were measured in the supernatant with the ATP bioluminescence kit (Roche diagnostics, Mannheim, Germany), and corrected for the total protein content of the sample estimated via the Lowry assay (Bio-Rad RC DC Protein Assay; Bio-Rad, Veenendaal, the Netherlands [32]).

Gene expression of fibrosis markers

To assess gene expression, total RNA was isolated, from pooled (n=3) and snap frozen slices, using an RNeasy Mini kit (Qiagen, Venlo, the Netherlands) according to the manufacturers recommendations. The amount of isolated RNA was measured with the ND-1000 spectrophotometer (Fisher Scientific, Landsmeer, the Netherlands), and 2 µg RNA was reversed transcribed using the Reverse Transcription System (Promega, Leiden, the Netherlands). The RT-PCR reaction was performed in the Eppendorf mastercycler gradient at 25 °C/10 minutes, 45 °C/60 minutes and 95 °C/5 minutes. The mRNA expression levels of heat shock protein 47 (HSP47), alpha smooth muscle actin (αSMA) and pro-collagen 1A1 (PCOL1A1) were detected using specific primer/probe sets (Table 3) and the qPCR master mix plus (Eurogentec, Maastricht, the Netherlands).

Table 3: Primers used in quantitative real-time PCR.

Gene	Forward	Reverse	Probe
HSP47	GCCCACCGTGGTGCCGCA	GCCAGGGCCGCCTCCAGGAG	CTCCCTCCTGCTTCTCAGCG
αSMA	AGGGGGTGATGGTGGGAA	ATGATGCCATGTTCTATCGG	GGGTGACGAAGCACAGAGCA
PCOL1A1	CAATCACCTGCGTACAGAACGCC	CGGCAGGGCTCGGGTTTC	CAGGTACCATGACCGAGACGTG
GAPDH	ACCAGGGCTGCTTTTAACTCT	GGTGCCATGGAATTTGCC	TGCCATCAATGACCCCTTCA
PDGF-BB	CTGGCATGCAAGTGTGAGAC	CGAATGGTCACCCGAGTTT	-
TGF-β1	GCAGCACGTGGAGCTGTA	CAGCCGGTTGCTGAGGTA	-
GAPDH	CGCTGGTGCTGAGTATGTCG	CTGTGGTCATGAGCCCTTCC	-

The Real-Time PCR reaction was performed using a 7900HT Real Time PCR (Applied Biosystems, Bleiswijk, the Netherlands) with 1 cycle of 95 °C/10 minutes and 45 cycles of 95 °C/15 seconds and 60 °C/1 minute. Gene expression levels of PDGF-BB and TGF-β1 were determined using the SYBR Green master mix (GC Biotech, Alphen aan den Rijn, the Netherlands) and specific primers (Table 3). The PCR reaction was performed using the same PCR system (see above) with 1 cycle of 95 ºC/10 minutes and 45 cycles of 95 ºC/15 seconds and 60 ºC/25 seconds followed by a dissociation curve (95 ºC/ 15 seconds: 60 ºC/15 seconds: 95 ºC/15 seconds). GAPDH was used as housekeeping gene and relative expression levels were calculated as fold change using the $2^{-\Delta\Delta CT}$ method.

Western blotting

Collagen 1 protein expression was determined by Western blot. Stored PCLS (see above) were lysed for 1h on ice in 250 µL RIPA buffer containing Protease inhibitor cocktail tablet (Boehringer Ingelheim, Alkmaar, the Netherlands), 50 mM Tris/HCl pH 7.5, 150 mM NaCl, 1% Igepal CA-630, 0.5% sodium deoxycholate and 0.1% SDS. The tissue was homogenized on ice by a Potter homogenizer and centrifuged (16,000 g) at 4 °C for 1h. Protein concentrations were determined in the supernatant using a Bio-Rad DC protein assay according to the manufacturer's protocol. Lysates were diluted 4-fold in SDS sample buffer (50 mM Tris/HCl pH 6.8, 2% SDS, 10% glycerol, 5% β-mercaptoethanol, 0.05% bromophenol blue) and boiled for 2 minutes. Next, 100 µg of protein was separated via SDS/PAGE using 7.5% gels and blotted onto an activated polyvinylidene difluoride membrane (Bio-Rad). Afterwards, the membrane was blocked using Tris-buffered saline supplemented with 5% Blocking Grade Powder (Bio-Rad) and 0.1% Tween-20 for 1h. Subsequently, membranes were incubated with rabbit-anti-collagen-1 (1:1000; Rockland, Gilbertsville, US) or mouse-anti-GAPDH (1:5000; Sigma). Binding of the antibody was determined using Horseradish Peroxidase and appropriate secondary and tertiary antibodies (Dako, Glostrup, Denmark). Protein levels were visualized with an imaging system using Western Lightning Plus-ECL (Perkin Elmer, Groningen, the Netherlands). Collagen protein expression was corrected for GAPDH levels and is displayed as relative values compared to the control.

Statistics

Three to five livers were used for each experiment, using triplicate slices from each liver. Results are expressed as means ± standard error of the mean (SEM). Statistical analysis was performed via non-parametric ANOVA followed by a Dunn's multiple comparisons test or using an unpaired two-tailed Student's *t*-test. A *p*-value of <0.05 was considered significant.

Results

Viability and expression profile of fibrosis markers in PCLS during culturing

As shown in Figure 1A, ATP levels of the untreated PCLS increase during the 1h preincubation as compared to the ATP values directly following slicing (0h). Moreover, the levels remain stable for at least 24h with an average ATP content of 7.3 ± 0.6 pmol/µg protein. After 48h of culturing, there is a small (28%) decrease of the ATP levels in untreated slices compared to 24h. Since there is a clear correlation between ATP content of the slices and viability as determined by morphological scoring (Figure 2; r=0.78, p=0.021), ATP levels can be used as a reliable viability marker. These results indicate that the viability of healthy PCLS could be sustained for 48h. Next, we studied the gene expression of several fibrosis markers (*e.g.* HSP47, αSMA and PCOL1A1) during culturing. Figure 1B demonstrates that the expression of HSP47 increases at all studied time points in healthy PCLS, PCOL1A1 levels were only elevated after 48h and αSMA expression was lower at all time points as compared to the gene level at 0h. Moreover, collagen 1 protein expression time-dependently increased 3-fold (24h) and 10-fold (48h) as compared to 0h (Figure 1C), in line with the observed PCOL1A1 gene levels. Quantitative PCR further revealed that after 48h of culture, PCOL1A1 expression in PCLS is similar to the level observed in slices prepared from cirrhotic tissue (Figure 1D). These findings illustrate the spontaneous induction of fibrogenesis in healthy PCLS, with HSP47 and PCOL1A1 serving as clear markers for this process. Therefore, these two genes were used as markers in the remainder of the study when evaluating the potency of anti-fibrotics.

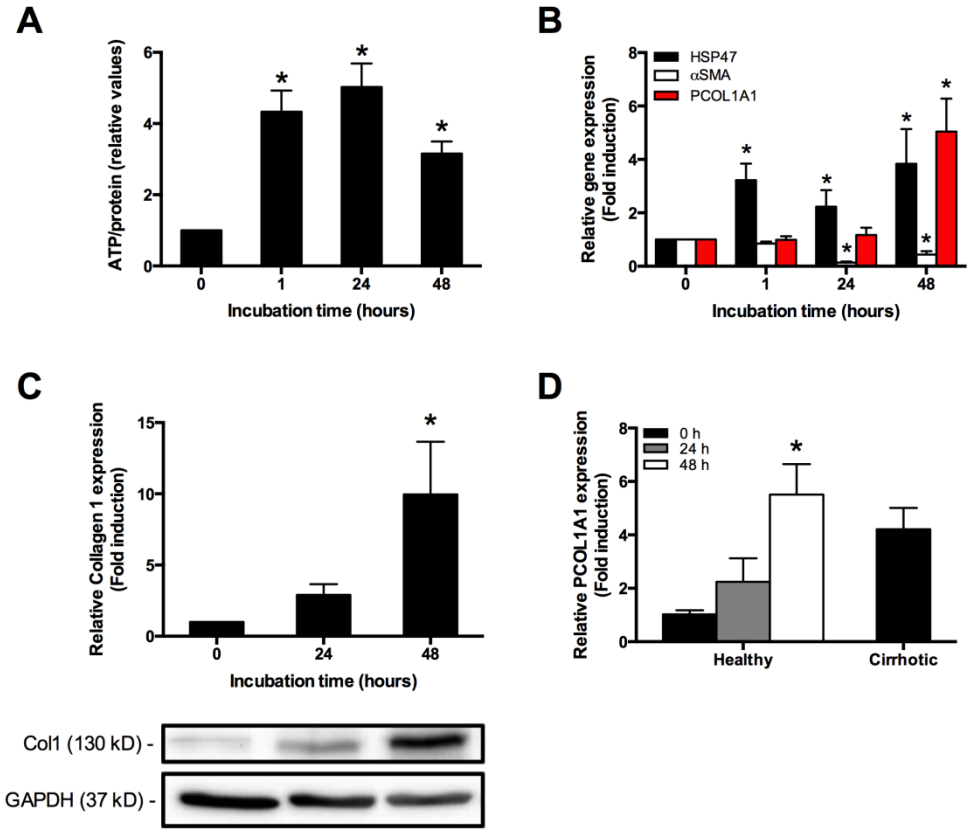

Figure 1: Viability of PCLS and expression of fibrosis markers. Human PCLS were cultured for 48h. (A) The viability of the slices was assessed by determining the ATP content (n=23). (B) After incubation, PCLS were collected and total mRNA was isolated. Afterwards, cDNA was synthesized and HSP47 (black bars; n=21), αSMA (white bars; n=7) and PCOL1A1 (red bars; n=21) gene expression was studied using qPCR. GAPDH was used as housekeeping gene and relative expression levels were calculated using the $2^{-\Delta\Delta CT}$ method. (C) Collagen 1 protein expression was studied by Western blotting. Proteins were separated via SDS/PAGE and blotted onto polyvinylidene difluoride membranes. Collagen was detected at 130 kD and GAPDH at 37 kD. Band intensities were corrected for GAPDH (n=3). (D) PCOL1A1 gene expression was studied in PCLS prepared from healthy and cirrhotic liver tissue using qPCR. GAPDH was used as housekeeping gene and relative expression levels were calculated using the $2^{-\Delta\Delta CT}$ method (n=3). Results are presented as means ± SEM of minimally three experiments performed in triplicate. *indicates $p<0.05$ compared to 0h.

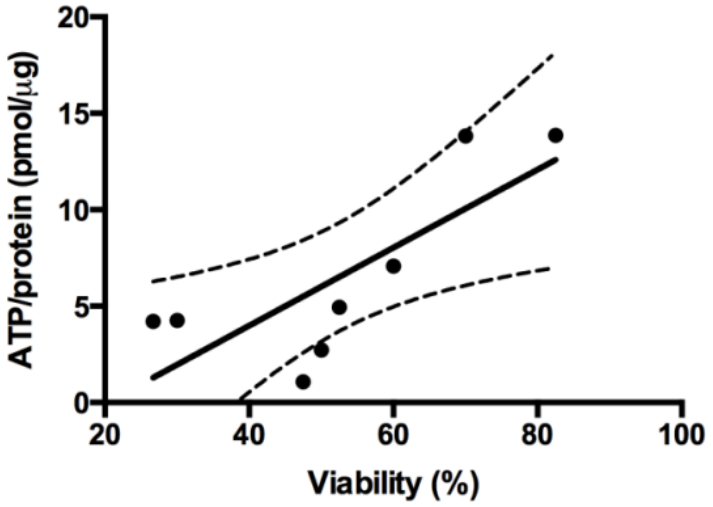

Figure 2: Viability of PCLS. Human PCLS were cultured for 3h. Afterwards, ATP levels were determined and viability was assessed by histomorphological examination. Pearson correlation analysis revealed a significant association between ATP and viability (r=0.78, p=0.021).

Pathways associated with the fibrogenic response in PCLS

Next, we investigated which pathway underlies the fibrotic response in human PCLS. After 48h of culturing, expression levels of both PDGF and TGF-β were significantly up-regulated compared to control (0h; Figure 3A), 6.2-fold and 2.7-fold, respectively. As shown in Figure 3B and 3C, addition of either growth factor could not significantly augment the fibrotic response in PCLS. Nevertheless, exposure of PCLS to a mixture of PDGF and TGF-β resulted in a significant induction of both HSP47 and PCOL1A1 gene expression as compared to control by 1.7-fold and 2.4-fold, respectively (Figure 3D). These results suggest that both pathways might contribute to the development of fibrosis in PCLS. This notion is corroborated by the observed reduction in HSP47 and PCOL1A1 gene expression following treatment with the MAPK inhibitor SB203580 (Figure 3E). In contrast, NSC23766 solely decreased HSP47 expression, while SIS3 had no effect.

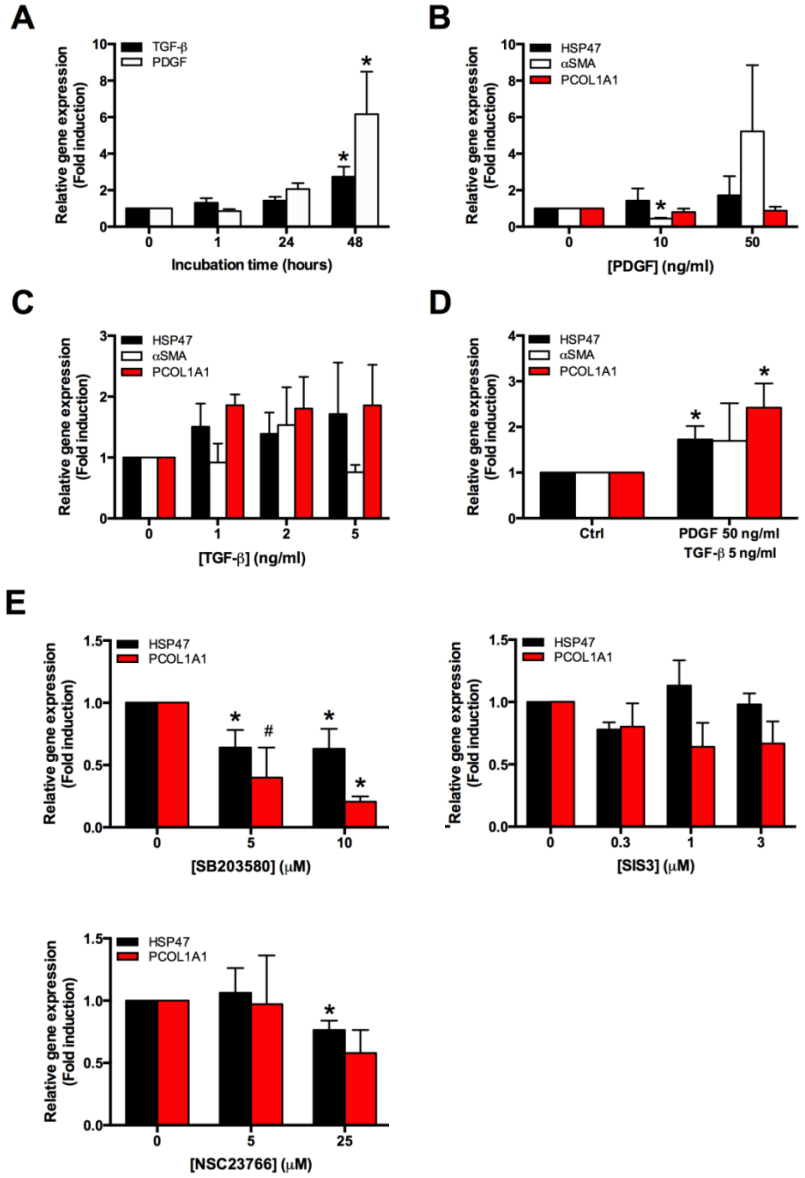

Figure 3: Pathways involved in fibrogenesis in human PCLS. Human PCLS were cultured for 48h in the presence or absence of PDGF, TGF-β or several inhibitors. Afterwards, gene expression was studied using qPCR. GAPDH was used as housekeeping gene and relative expression levels were calculated using the $2^{-\Delta\Delta CT}$ method. (A) Gene expression of TGF-β (black bars) or PDGF (white bars) in human PCLS during culturing (n=5). Impact of (B) PDGF (n=4), (C) TGF-β (n=4) or (D) PDGF + TGF-β (n=5) on the gene expression of HSP47 (black bars), αSMA (white bars) and PCOL1A1 (red bars) in PCLS. (E) Impact of several inhibitors on the gene expression of HSP47 (black bars) and PCOL1A1 (red bars) in PCLS (n=4). Results are presented as means ± SEM of minimally three experiments performed in triplicate. *indicates $p<0.05$, #indicates $p=0.059$.

Impact of anti-fibrotic drugs on the gene expression of fibrosis markers

Since both the PDGF and TGF-β pathway appear to induce fibrogenesis in human PCLS, we investigated the capacity of multiple potential anti-fibrotic compounds, associated with either pathway, to mitigate the observed increase in expression of the fibrosis markers. The inhibitors mainly targeting the PDGF pathway were not toxic for PCLS at the tested concentrations, except for the highest concentration of imatinib (10 µM; Figure 4A). Quantitative PCR revealed that sunitinib, in a concentration range of 0.5 µM to 5 µM, reduced the gene expression of HSP47 and PCOL1A1 with more than 27%, and up to 65%, compared to the control slices incubated for 48h without inhibitor, whereas, imatinib and sorafenib did not influence the gene expression of both markers (Figure 4B).

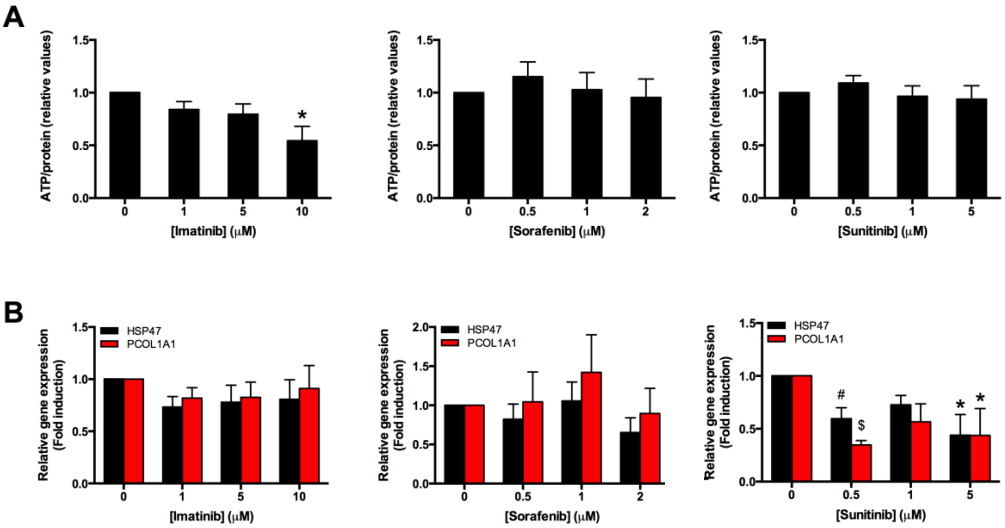

Figure 4: Impact of PDGF-inhibitors on human PCLS. Human PCLS were treated with different PDGF-inhibitors for 48h. (A) The viability of the slices was assessed by determining the ATP content (n=4). (B) After treatment, PCLS were collected and total mRNA was isolated. Afterwards, cDNA was synthesized and HSP47 (black bars) and PCOL1A1 (red bars) gene expression was studied using qPCR (n=5). GAPDH was used as housekeeping gene and relative expression levels were calculated using the $2^{-\Delta\Delta CT}$ method. Results are presented as means ± SEM of minimally three experiments performed in triplicate. *indicates $p<0.05$, #indicates $p=0.074$, $indicates $p=0.056$.

Regarding the TGF-β-inhibitors, toxicity was only observed for pirfenidone at the highest concentrations tested (2.5 mM) illustrated by a reduction in ATP levels of more than 30% (Figure 5A). As shown in Figure 5B, 0.5 mM valproic acid decreased the expression level of both HSP47 and PCOL1A1 with 64% and 43%, respectively, while rosmarinic acid, tetrandrine and pirfenidone reduced the gene expression of PCOL1A1 but not that of HSP47. In contrast, perindopril did not affect gene expression levels of any of the fibrosis markers. Thus, both classes of anti-fibrotic compounds can influence fibrogenesis in PCLS, yet the TGF-β-inhibitors seem to be more effective than the PDGF-inhibitors.

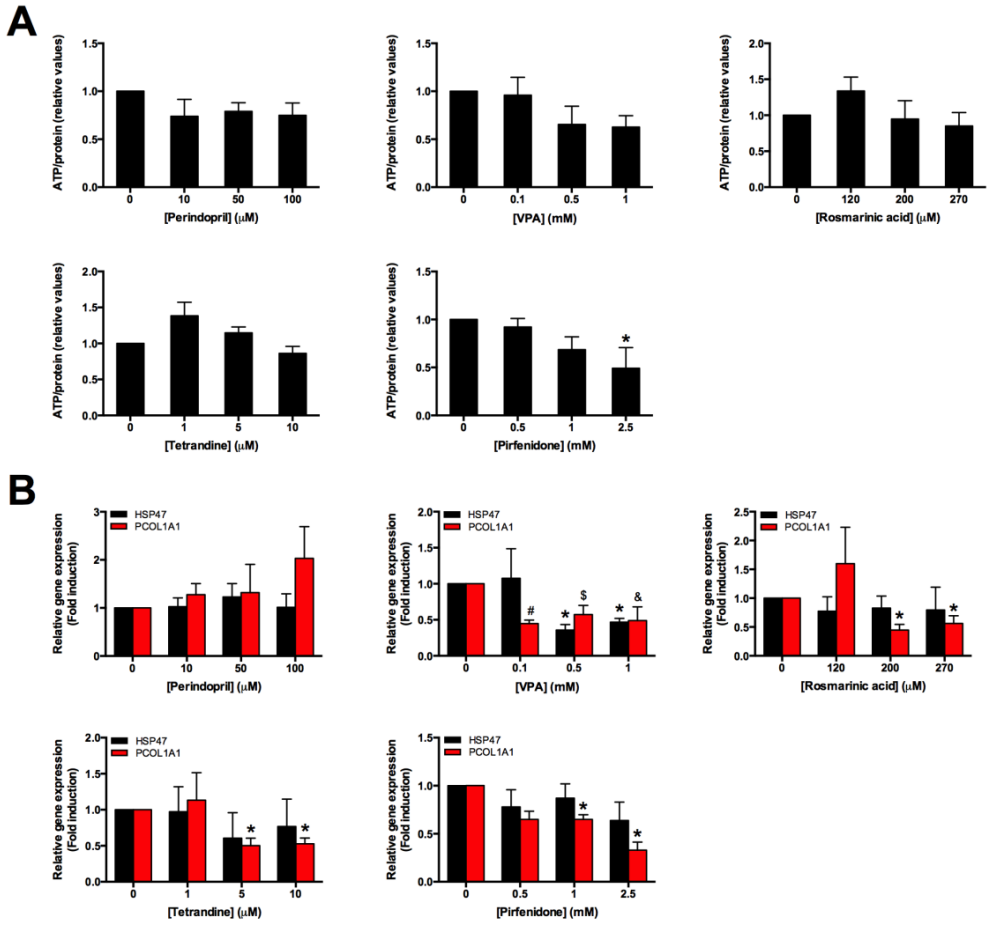

Figure 5: Impact of TGF-β-inhibitors on human PCLS. Human PCLS were treated with different TGF-β-inhibitors for 48h. (A) Viability of the slices was assessed by determining the ATP content (n=4). (B) After treatment, PCLS were collected and total mRNA was isolated. Afterwards, cDNA was synthesized and HSP47 (black bars) and PCOL1A1 (red bars) gene expression was studied using qPCR (n=4). GAPDH was used as housekeeping gene and relative expression levels were calculated using the $2^{-\Delta\Delta CT}$ method. Results are presented as means ± SEM of minimally three experiments performed in triplicate. *indicates $p<0.05$, #indicates $p=0.063$, $indicates $p=0.055$, &indicates $p=0.075$.

Discussion

Here, we describe the onset and molecular mechanism of fibrosis in healthy human PCLS. In addition, we evaluated the antifibrotic efficacy of a broad range of different compounds using this unique model. The expected therapeutic targets of the tested compounds and the obtained results are summarized in Figure 6.

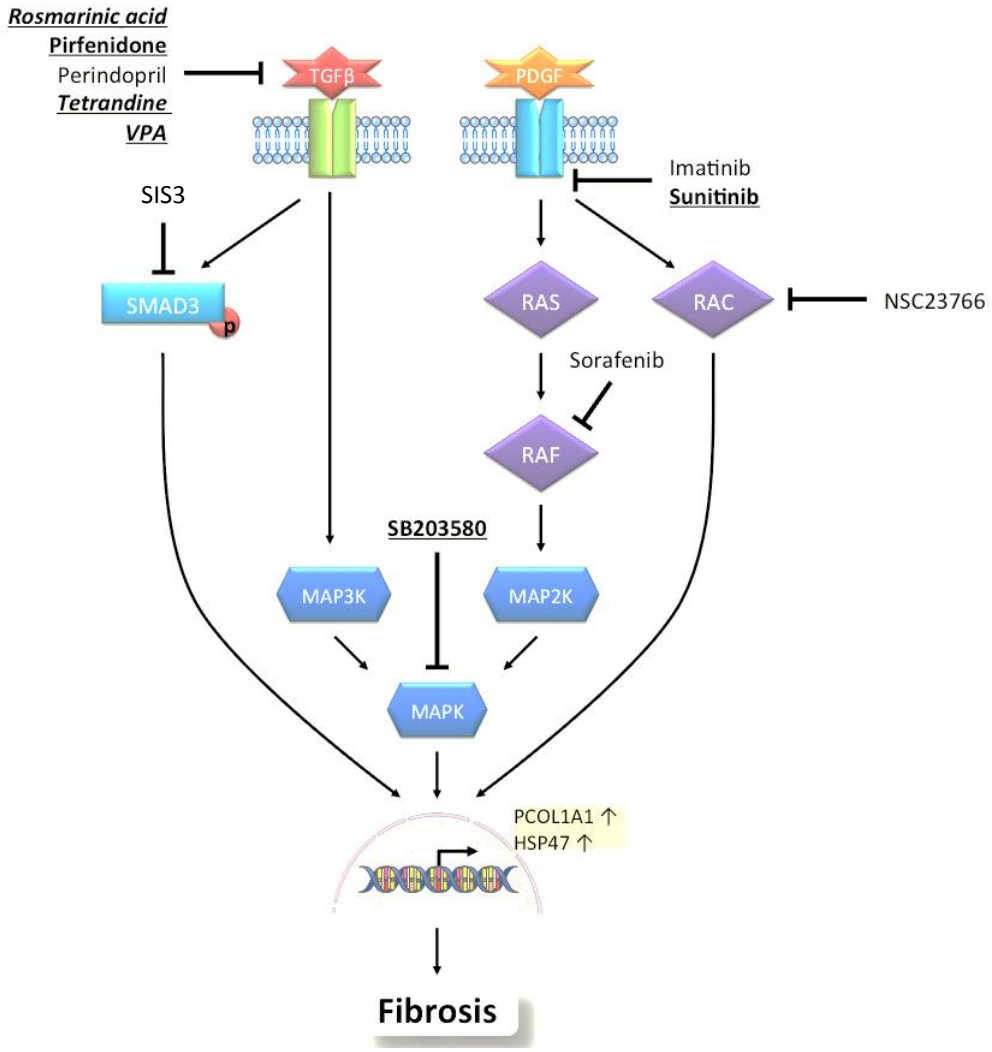

Figure 6: Overview of drug targets and efficacy of the tested compounds in PCLS. Schematic overview of the expected drug targets. Compounds that show anti-fibrotic effects in our model are emphasized in bold and underline. Compounds for which the molecular targets are not fully elucidated are presented in italic.

In this study, we report the early onset of fibrosis in healthy human PCLS during culturing, as illustrated by a clear increase in the gene expression of both HSP47 and PCOL1A1. However, the fibrotic process in human PCLS was not associated with an increased expression of the well-known fibrosis and myofibroblast marker αSMA [33]. The observed gene expression profile is in agreement with a previous study from our group using human PCLS [34]. As suggested previously, the decrease of αSMA expression might indicate a loss of myofibroblasts in human PCLS, since fibulin-2 expression also decreased while gene levels of the hepatic stellate cell marker, synaptophysin, remained stable during culturing [34]. Although PCLS represent a good and multicellular model for fibrotic disease, the specific role of myofibroblasts in this model requires further study.

As mentioned before, there are clear species differences in the fibrotic process as well as the effectiveness of anti-fibrotic compounds. For instance, using rat PCLS, we previously demonstrated that the early onset of fibrogenesis in this rodent model was accompanied by an increased gene expression of HSP47, PCOL1A1 and αSMA [7]. Moreover, contrary to the current study, expression of these markers could be augmented in rat PCLS by treatment with either PDGF or TGF-β [7]. With regard to anti-fibrotic compounds, we now report that TGF-β pathway inhibitors are more effective in dampening fibrosis in human PCLS as compared to PDGF-inhibitors. This is in disparity to rat PCLS, where the early onset of fibrosis could be more effectively countered with PDGF pathway inhibitors [7]. These results might explain why several drugs, with proven anti-fibrotic effects in animal studies, lack efficacy in man. To illustrate, imatinib, a well-known PDGF receptor tyrosine kinase inhibitor [35], was demonstrated to be a potent anti-fibrotic compound in a broad array of rodent fibrosis models affecting several organs such as the lung, kidney and liver [7, 8, 36-38]. Moreover, imatinib has been shown to induce apoptosis of hepatic stellate cells *in vitro* [39]. Yet, in the current study, imatinib was ineffective as anti-fibrotic compound in human PCLS. This finding is in agreement with a randomized double-blind clinical trial showing that the compound was ineffective as anti-fibrotic drug in humans, since the compound did not affect survival or lung function in patients with idiopathic pulmonary fibrosis [40]. In addition, it is well known that imatinib can induce hepatotoxicity [41, 42], similar to our observations in human PCLS. Taken together, it is clear that there are species-specific effects of potential anti-fibrotic compounds, further illuminating the pressing need for reliable and reproducible human *in vitro* fibrosis models for, among others, drug development.

Our results further demonstrate that pirfenidone, valproic acid and rosmarinic acid, among others, had a clear impact on the gene expression of fibrosis markers in human PCLS. These results are in line with our previous observations in rodent PCLS [7, 9]. Pirfenidone is a well-established anti-fibrotic compound shown to reduce TGF-β expression in a wide variety of animal models of fibrosis [43]. Also, using human LX-2 cells, it was shown that pirfenidone diminished αSMA and COL1 gene expression [44]. Furthermore, Armendariz-Borunda *et al.* reported that twelve months of pirfenidone treatment caused a reduction in both the gene and protein expression of COL1A, TGF-β and tissue inhibitors of metalloproteinases (TIMP)-1 in liver biopsies from patients with advanced liver fibrosis [45]. Moreover, treatment with pirfenidone was also demonstrated to be beneficial in patients with diabetic nephropathy and idiopathic pulmonary fibrosis [46, 47]. Yet, in our hands, toxicity was observed with the highest tested concentration of pirfenidone, although this did not result in a reduction of HSP47 gene expression. Therefore, the true anti-fibrotic potential of pirfenidone requires further scrutiny; nevertheless, the compound shows great potential as a therapeutic agent against fibrotic diseases in humans, partially supported by our results in human PCLS.

Valproic acid, an anti-epileptic drug that possess histone deacetylase (HDAC) inhibitory activity, markedly decreased gene expression of fibrosis markers in human PCLS, although this effect might be due to hepatotoxicity, since a non-significant decrease of ATP content was observed at concentrations ≥0.5 mM. Nonetheless, at the lowest concentration we also observed a clear reduction in PCOL1A1 gene levels. This suggests that valproic acid might be useful as anti-fibrotic drug. This notion is supported by the study of Watanabe *et al*. showing that valproic acid diminished TFG-β-induced collagen 1A1 gene and protein expression, as well as the number of αSMA fibers in LI90 cells [48]. These results warrant further investigation into the use HDAC inhibitors for the treatment of (liver) fibrosis.

Rosmarinic acid is a caffeic acid ester present in a myriad of plants [49]. Several studies report anti-fibrotic effects of this compound [50-52]. Yet, to the best of our knowledge, our study is the first to report the anti-fibrotic properties of rosmarinic acid using a human fibrosis model. Previously, we demonstrated that rosmarinic acid decreased the expression of fibrosis markers in fibrotic rat PCLS as well as healthy murine PCLS [7-9]. Therefore, we postulate that anti-fibrotic effects of rosmarinic acid in human liver fibrosis may be expected.

Next to testing the efficacy of anti-fibrotics in human PCLS, we also strove to unravel the molecular pathways underlying fibrogenesis in the model. Our results indicated that the MAPK pathway plays a vital role during the onset of the fibrotic process in human PCLS, in agreement with our observations in rat PCLS (unpublished data). This notion is further supported by the study from Varela-Rey *et al.* demonstrating that the specific p38-MAPK inhibitor SB203580 abated the induction of COL1A1 gene expression by TGF-β in hepatic stellate cells [53]. In addition, our findings suggested that induction of fibrosis in human PCLS by TGF-β goes via the MAPK pathway and is independent of SMAD3. The SMAD-independent activity of both pathways in regulating collagen gene expression has been reported before by Tsukada and colleagues [22]. The trigger for MAPK activation in human PCLS remains unclear. It is known that this pathway can be induced by reactive oxygen species (ROS) [54], and even though PCLS are cultured in an atmosphere with high oxygen levels, prior literature demonstrated that there is no evidence for the presence of ROS in the model [55-57]. Moreover, previous work from our group revealed that accumulation of waste products or bile salts is not involved in the observed fibrotic response in PCLS [34]. Thus, the causative agent(s) for fibrogenesis by culture activation in human PCLS remain to be elucidated. Of note, culture conditions have a profound impact on PCLS and should be tailored to fit the study type (*e.g.* drug metabolism or toxicity) [58].

The current study only delineated the pathways underlying the early onset of fibrosis in human PCLS as well as the efficacy of anti-fibrotic compounds during this stage of the disease process. To gain more insight in the complete pathophysiological mechanism of liver fibrosis, studies are currently underway using PCLS prepared from human cirrhotic livers. These studies will hopefully grant us a better understanding of fibrotic disease and provide new leads for therapeutic targets.

In conclusion, in this study we demonstrate that TGF-β pathway inhibitors effectively hamper incipient fibrosis in human PCLS. Moreover, it became apparent that the MAPK signaling cascade plays a vital role in the fibrotic process. Our results provide additional insight into the mechanism of liver fibrosis and establish human PCLS as a good model for this disease.

Acknowledgements

The authors would like to thank all the transplantation coordinators and surgeons at the UMCG for providing human liver samples. We also thank Marina de Jager, Miriam Langelaar-Makkinje, Marjolijn Merema, Sylvia Blomsma and Patricia Robbe for their help with preparing human PCLS, and Inge de Graaf for histomorphological scoring. This work was supported by ZonMw (Program: Dierproeven begrensd II, project 114000098).

References

1. Zeisberg, M. and R. Kalluri, Cellular mechanisms of tissue fibrosis. 1. Common and organ-specific mechanisms associated with tissue fibrosis. Am J Physiol Cell Physiol, 2013. 304(3): p. C216-25.
2. Pellicoro, A., et al., Liver fibrosis and repair: immune regulation of wound healing in a solid organ. Nat Rev Immunol, 2014. 14(3): p. 181-94.
3. Schuppan, D. and Y.O. Kim, Evolving therapies for liver fibrosis. J Clin Invest, 2013. 123(5): p. 1887-901.
4. Westra, I.M., et al., Evaluation of fibrosis in precision-cut tissue slices. Xenobiotica, 2013. 43(1): p. 98-112.
5. Stribos, E.G., et al., Precision-cut human kidney slices as a model to elucidate the process of renal fibrosis. Transl Res, 2015.
6. van de Bovenkamp, M., et al., Precision-cut fibrotic rat liver slices as a new model to test the effects of anti-fibrotic drugs in vitro. J Hepatol, 2006. 45(5): p. 696-703.
7. Westra, I.M., et al., Precision-cut liver slices as a model for the early onset of liver fibrosis to test antifibrotic drugs. Toxicol Appl Pharmacol, 2014. 274(2): p. 328-38.
8. Westra, I.M., et al., The effect of antifibrotic drugs in rat precision-cut fibrotic liver slices. PLoS One, 2014. 9(4): p. e95462.
9. Iswandana, R., et al., Organ- and species-specific biological activity of rosmarinic acid. Toxicol In Vitro, 2016. 32: p. 261-268.
10. Bonner, J.C., Regulation of PDGF and its receptors in fibrotic diseases. Cytokine Growth Factor Rev, 2004. 15(4): p. 255-73.
11. Parsons, C.J., M. Takashima, and R.A. Rippe, Molecular mechanisms of hepatic fibrogenesis. J Gastroenterol Hepatol, 2007. 22 Suppl 1: p. S79-84.
12. Liu, Y., et al., Animal models of chronic liver diseases. Am J Physiol Gastrointest Liver Physiol, 2013. 304(5): p. G449-68.
13. Inoue, T., et al., The contribution of epithelial-mesenchymal transition to renal fibrosis differs among kidney disease models. Kidney Int, 2015. 87(1): p. 233-8.
14. Liu, Y., Cellular and molecular mechanisms of renal fibrosis. Nat Rev Nephrol, 2011. 7(12): p. 684-96.
15. Jinnin, M., H. Ihn, and K. Tamaki, Characterization of SIS3, a novel specific inhibitor of Smad3, and its effect on transforming growth factor-beta1-induced extracellular matrix expression. Mol Pharmacol, 2006. 69(2): p. 597-607.
16. Gao, Y., et al., Rational design and characterization of a Rac GTPase-specific small molecule inhibitor. Proc Natl Acad Sci U S A, 2004. 101(20): p. 7618-23.
17. Cuenda, A., et al., Sb-203580 is a specific inhibitor of a Map kinase homolog which is stimulated by cellular stresses and interleukin-1. Febs Letters, 1995. 364(2): p. 229-233.
18. Elferink, M.G., et al., Gene expression analysis of precision-cut human liver slices indicates stable expression of ADME-Tox related genes. Toxicol Appl Pharmacol, 2011. 253(1): p. 57-69.
19. van de Bovenkamp, M., et al., Human liver slices as an in vitro model to study toxicity-induced hepatic stellate cell activation in a multicellular milieu. Chemico-biological interactions, 2006. 162(1): p. 62-69.
20. de Graaf, I.A., et al., Preparation and incubation of precision-cut liver and intestinal slices for application in drug metabolism and toxicity studies. Nat Protoc, 2010. 5(9): p. 1540-51.
21. Olinga, P., et al., Effect of cold and warm ischaemia on drug metabolism in isolated hepatocytes and slices from human and monkey liver. Xenobiotica, 1998. 28(4): p. 349-60.
22. Tsukada, S., et al., SMAD and p38 MAPK signaling pathways independently regulate alpha1(I) collagen gene expression in unstimulated and transforming growth factor-beta-stimulated hepatic stellate cells. J Biol Chem, 2005. 280(11): p. 10055-64.
23. Xu, S.W., et al., Rac inhibition reverses the phenotype of fibrotic fibroblasts. PLoS One, 2009. 4(10): p. e7438.
24. Leveque, D. and F. Maloisel, Clinical pharmacokinetics of imatinib mesylate. In vivo (Athens, Greece), 2005. 19(1): p. 77-84.
25. Strumberg, D., et al., Safety, pharmacokinetics, and preliminary antitumor activity of sorafenib: a review of four phase I trials in patients with advanced refractory solid tumors. The oncologist, 2007. 12(4): p. 426-437.
26. Minkin, P., et al., Quantification of sunitinib in human plasma by high-performance liquid chromatography-tandem mass spectrometry. Journal of chromatography.B, Analytical technologies in the biomedical and life sciences, 2008. 874(1-2): p. 84-88.
27. Devissaguet, J.P., et al., Pharmacokinetics of perindopril and its metabolites in healthy volunteers. Fundam Clin Pharmacol, 1990. 4(2): p. 175-89.
28. Chavez-Blanco, A., et al., Histone acetylation and histone deacetylase activity of magnesium valproate in tumor and peripheral blood of patients with cervical cancer. A phase I study. Mol Cancer, 2005. 4(1): p. 22.
29. Rubino, C.M., et al., Effect of food and antacids on the pharmacokinetics of pirfenidone in older healthy adults. Pulm Pharmacol Ther, 2009. 22(4): p. 279-85.

30. de Graaf, I.A., et al., Increased post-thaw viability and phase I and II biotransformation activity in cryopreserved rat liver slices after improvement of a fast-freezing method. Drug Metab Dispos, 2000. 28(9): p. 1100-6.
31. Hadi, M., et al., Human precision-cut liver slices as an ex vivo model to study idiosyncratic drug-induced liver injury. Chem Res Toxicol, 2013. 26(5): p. 710-20.
32. Lowry, O.H., et al., Protein measurement with the Folin phenol reagent. J Biol Chem, 1951. 193(1): p. 265-75.
33. Hinz, B., et al., Recent developments in myofibroblast biology: paradigms for connective tissue remodeling. Am J Pathol, 2012. 180(4): p. 1340-55.
34. van de Bovenkamp, M., et al., Liver slices as a model to study fibrogenesis and test the effects of anti-fibrotic drugs on fibrogenic cells in human liver. Toxicol In Vitro, 2008. 22(3): p. 771-8.
35. Buchdunger, E., et al., Abl protein-tyrosine kinase inhibitor STI571 inhibits in vitro signal transduction mediated by c-kit and platelet-derived growth factor receptors. J Pharmacol Exp Ther, 2000. 295(1): p. 139-45.
36. Daniels, C.E., et al., Imatinib mesylate inhibits the profibrogenic activity of TGF-beta and prevents bleomycin-mediated lung fibrosis. J Clin Invest, 2004. 114(9): p. 1308-16.
37. Wang, S., et al., Imatinib mesylate blocks a non-Smad TGF-beta pathway and reduces renal fibrogenesis in vivo. FASEB J, 2005. 19(1): p. 1-11.
38. Yoshiji, H., et al., Imatinib mesylate (STI-571) attenuates liver fibrosis development in rats. Am J Physiol Gastrointest Liver Physiol, 2005. 288(5): p. G907-13.
39. Kuo, W.L., et al., Imatinib mesylate improves liver regeneration and attenuates liver fibrogenesis in CCL4-treated mice. J Gastrointest Surg, 2012. 16(2): p. 361-9.
40. Daniels, C.E., et al., Imatinib treatment for idiopathic pulmonary fibrosis: Randomized placebo-controlled trial results. Am J Respir Crit Care Med, 2010. 181(6): p. 604-10.
41. Mindikoglu, A.L., et al., Imatinib mesylate (gleevec) hepatotoxicity. Dig Dis Sci, 2007. 52(2): p. 598-601.
42. Lyseng-Williamson, K. and B. Jarvis, Imatinib. Drugs, 2001. 61(12): p. 1765-74; discussion 1775-6.
43. Schaefer, C.J., et al., Antifibrotic activities of pirfenidone in animal models. Eur Respir Rev, 2011. 20(120): p. 85-97.
44. Zhao, X.Y., et al., Pirfenidone inhibits carbon tetrachloride- and albumin complex-induced liver fibrosis in rodents by preventing activation of hepatic stellate cells. Clin Exp Pharmacol Physiol, 2009. 36(10): p. 963-8.
45. Armendariz-Borunda, J., et al., A pilot study in patients with established advanced liver fibrosis using pirfenidone. Gut, 2006. 55(11): p. 1663-5.
46. Sharma, K., et al., Pirfenidone for diabetic nephropathy. J Am Soc Nephrol, 2011. 22(6): p. 1144-51.
47. King, T.E., Jr., et al., A phase 3 trial of pirfenidone in patients with idiopathic pulmonary fibrosis. N Engl J Med, 2014. 370(22): p. 2083-92.
48. Watanabe, T., et al., Sodium valproate blocks the transforming growth factor (TGF)-beta1 autocrine loop and attenuates the TGF-beta1-induced collagen synthesis in a human hepatic stellate cell line. Int J Mol Med, 2011. 28(6): p. 919-25.
49. Petersen, M., et al., Evolution of rosmarinic acid biosynthesis. Phytochemistry, 2009. 70(15-16): p. 1663-79.
50. Li, G.S., et al., In vitro and in vivo antifibrotic effects of rosmarinic acid on experimental liver fibrosis. Phytomedicine, 2010. 17(3-4): p. 282-8.
51. Zhang, J.J., et al., Rosmarinic acid inhibits proliferation and induces apoptosis of hepatic stellate cells. Biol Pharm Bull, 2011. 34(3): p. 343-8.
52. Domitrovic, R., et al., Rosmarinic acid ameliorates acute liver damage and fibrogenesis in carbon tetrachloride-intoxicated mice. Food Chem Toxicol, 2013. 51: p. 370-8.
53. Varela-Rey, M., et al., p38 MAPK mediates the regulation of alpha1(I) procollagen mRNA levels by TNF-alpha and TGF-beta in a cell line of rat hepatic stellate cells(1). FEBS letters, 2002. 528(1-3): p. 133-138.
54. Adachi, T., et al., NAD(P)H oxidase plays a crucial role in PDGF-induced proliferation of hepatic stellate cells. Hepatology, 2005. 41(6): p. 1272-81.
55. Schaffert, C.S., et al., Exposure of precision-cut rat liver slices to ethanol accelerates fibrogenesis. American journal of physiology.Gastrointestinal and liver physiology, 2010. 299(3): p. G661-8.
56. Klassen, L.W., et al., An in vitro method of alcoholic liver injury using precision-cut liver slices from rats. Biochemical pharmacology, 2008. 76(3): p. 426-436.
57. Vickers, A.E., et al., Organ slice viability extended for pathway characterization: an in vitro model to investigate fibrosis. Toxicological sciences : an official journal of the Society of Toxicology, 2004. 82(2): p. 534-544.
58. Starokozhko, V., et al., Viability, function and morphological integrity of precision-cut liver slices during prolonged incubation: Effects of culture medium. Toxicol In Vitro, 2015. 30(1 Pt B): p. 288-99.

Supplementary box III

Free radicals

- A free radical can be defined as an atom, molecule or ion that has an unpaired valence electron. Free radicals are highly chemically reactive and spontaneously interact with neighboring molecules thereby causing damage to key cellular components [1].
- Reactive oxygen species (ROS) are free radicals that contain oxygen in the molecule such as peroxides, superoxide, hydroxyl radical and singlet oxygen. Excessive production of ROS can cause oxidative stress [2].
- Reactive nitrogen species (RNS) are nitric oxide-derived free radicals such as peroxynitrite, nitrous oxide, nitrogen dioxide and dinitrogen trioxide. Uncontrolled production of RNS is called nitrosative stress [3].
- ROS and RNS usually act together to damage cells, and oxidative/nitrosative stress is a significant contributor to numerous disorders [4].

1. Lobo, V., et al., Free radicals, antioxidants and functional foods: Impact on human health. Pharmacognosy Reviews, 2010. 4(8): p. 118-126.
2. Pham-Huy, L.A., H. He, and C. Pham-Huy, Free radicals, antioxidants in disease and health. International Journal of Biomedical Science : IJBS, 2008. 4(2): p. 89-96.
3. Martinez, M.C. and R. Andriantsitohaina, Reactive nitrogen species: molecular mechanisms and potential significance in health and disease. Antioxid Redox Signal, 2009. 11(3): p. 669-702.
4. Adams, L., M.C. Franco, and A.G. Estevez, Reactive nitrogen species in cellular signaling. Experimental Biology and Medicine, 2015. 240(6): p. 711-717.